Kinetic Investigation of Self-Condensing Group Transfer Polymerization

Peter F. W. Simon and Axel H. E. Müller*

Makromolekulare Chemie II and Bayreuther Institut für Makromolekülforschung, Universität Bayreuth, D-95440 Bayreuth, Germany

Received December 11, 2003; Revised Manuscript Received June 13, 2004

ABSTRACT: Hyperbranched methacrylates were synthesized by self-condensing group transfer polymerization (SCGTP) of 2-(2-methyl-1-triethylsiloxy-1-propenyloxy)ethyl methacrylate (MTSHEMA) and characterized by multidetector SEC and ^{13}C NMR. Depending on the reaction conditions, molecular weights up to $M_w = 38\,000$ at a polydispersity of $M_w/M_n \approx 3.8$ could be obtained. Kinetic measurements showed that cyclization, i.e., the intramolecular reaction of a functional group with the polymer's vinyl group, limits the molecular weights and lowers the polydispersity. A maximum degree of branching of $DB \approx 0.4$ and a reactivity ratio of the propagating and initiating groups in the range of $13 < r < 23$ were determined. Slow addition of MTSHEMA to the monofunctional initiator, 1-methoxy-3-(trimethylsilyloxy)-2-methyl-1-propene (MTS), enabled the control of molecular weights and decreased the polydispersity to $M_w/M_n \approx 2.8$. The addition of methyl methacrylate (MMA) to a living MTSHEMA core yielded a "hyperstar" polymer.

Introduction

During the past decade, interest in hyperbranched polymers has increased.[1−5] They combine some features of a dendritic architecture, e.g., an increasing number of end groups and a globular structure in solution, with the ease of preparation of a linear polymer by means of a one-pot reaction.[6,7]

Hyperbranched vinyl polymers became accessible using a technique named self-condensing vinyl polymerization (SCVP) of initiator monomers.[8] These are of a general AB* type structure, where A stands for a polymerizable vinyl group and B* represents a group capable of initiating the polymerization of the A-type functionalities. Thus, this species combines features of an *ini*tiator and a mono*mer* and has therefore been named "inimer" (cf. Chart 1).[9−12] Consequently, this approach is analogous to the case of an AB_2-type monomer which was discussed by Flory.[1] As the reaction between the same functional groups is not possible, the polyreaction of both types results in highly branched polymers without any network formation.

The growth of the polymer in SCVP is initiated by addition of the active B* group to the vinyl group of another inimer. The vinyl group, A, of the second inimer is then converted into a new active group, A*. The dimer formed has two active sites, A* and B*, one double bond, A, and one inactive group, b, stemming from the initiating moiety of the first inimer. Both the initiating B* moiety and the newly created propagating group, A*, can react with the vinyl group, A, of any other molecule (inimer or polymer) in an analogous way with rate constants k_A and k_B, respectively. To find a short representation for the different groups, we use capital letters for the vinyl group (A) and for active moieties (A*, B*) and lowercase letters for reacted ones (a, b) (cf. Scheme 1).

Self-condensing vinyl polymerization has been applied to various types of living polymerization, i.e., cationic,[8] ATRP,[13−18] nitroxide-mediated radical polymerization,[19] and even ring-opening polymerization.[20] Baskaran employed an anionic route to hyperbranched styrene derivatives by reacting an equimolar amount of 1,3-diisopropylbenzene and *n*-butyllithium, thus forming an inimer in situ.[21] We[22]—and independently Sakamoto et al.[23]—have used group transfer polymerization (GTP) of the inimer 2-(2-methyl-1-triethylsiloxy-1-propenyloxy)-ethyl methacrylate (MTSHEMA) **(1)** (cf. Chart 1) where the silylketene acetal group can be activated by nucleophilic catalysts to initiate GTP.[24,25]

Chart 1

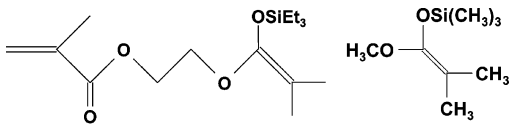

MTSHEMA **(1)** *INIMER* MTS **(2)** *INITIATOR*

The molecular weights of hyperbranched polymers are limited by cyclization. In this inevitable reaction an active chain end reacts intramolecularly with the double bond, forming a macroinitiator containing one loop. Clearly, this loop should only have a minor effect on the physical properties; however, it will significantly narrow the molecular weight distribution of the polymer formed.[26−28] An approach to further narrow down the molecular weight distribution of a hyperbranched polymer was outlined in theoretical and experimental work.[27,29−31] Employing an *f*-functional initiator, G_f, which lacks a double bond and only contains initiating B* moieties, enables control over the molecular weight distribution in SCVP. Furthermore, structural control can be increased if the inimer is added slowly (semi-batch conditions).

According to theoretical considerations, differences in reactivity of the initiating and propagating groups, A* and B*, respectively, strongly influence the polydispersity as well as the degree of branching.[11,32] If the polymerization mechanism is based on a dynamic equilibration between active and dormant (covalent) species, the deactivation process of one type of groups may not be fast enough. Consequently, linear growth might occur several times before the deactivation takes place. The apparent reactivity increase of the A* or B*

* Corresponding author: Fax +49-921-553393, e-mail axel.mueller@uni-bayreuth.de.

10.1021/ma0358834 CCC: $27.50
Published on Web 09/11/2004

Scheme 1. A Possible Hexamer of MTSHEMA after Protonation (Marked with H) and Different Types of Its Representation (from Upper Left to Lower Right): Structural Units, Functional Groups, and Chemical Structure

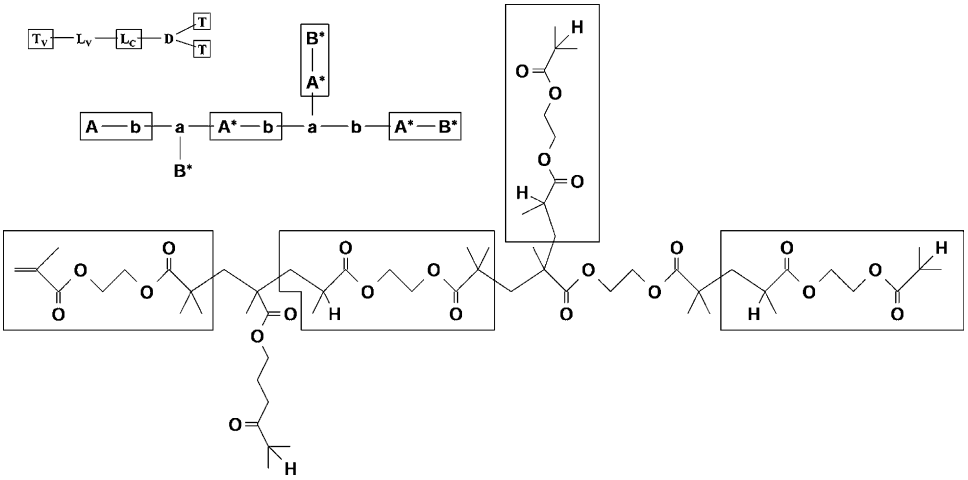

Table 1. Structural Units and Functional Groups in the Self-Condensing Group Transfer Polymerization

structural unit	functional group	description
D	ab and $a_{cyc}b$[a]	branch point
L_C	A*b	linear (polycondensate type)
L_V	aB* and $a_{cyc}B^*$ [a]	linear (vinyl type)
T_V	Ab	terminal (vinyl type)
T	A*B*	terminal

[a] The a_{cyc} group is generated in the backbiting reaction (vide infra).

group causes an enhanced proportion of one type of these moieties. Thus, although chemically both A* and B* may have very similar intrinsic reactivities ($k_A \approx k_B$), the slow deactivation process may apparently consume one active group faster.[16] Hence, a variation of the reaction conditions in the self-condensing group transfer polymerization (SCGTP) of MTSHEMA **(1)** may lead to differences in the molecular weight distribution as well as in the architecture of the hyperbranched polymer.[32]

When considering the structure of hyperbranched macromolecules, it is more useful to discuss the connectivity of the structural units rather than functional groups. Structural units are composed of a combination of two unlike functional groups (cf. Table 1). In Scheme 1, one out of many possible structures of a hyperbranched MTSHEMA **(1)** hexamer after termination with protons is sketched, and the different representations (functional groups and structural units) are outlined.

In the hexamer depicted in Scheme 1 six different types of structural units can be found. The terminal unit, T, is made of two active functional groups (A* and B*). The T_V unit consists of a vinyl group, A, and one reacted initiating group, b. The branched ("dendritic") unit, D, is composed of two inactive groups (a and b). Furthermore, the existence of two different types of linear units, L_V and L_C, is evident, leading to two different linear analogues (cf. Scheme 2 and Table 1). One of these linear polymers is composed of L_V units resembling a vinyl polymer. Such a macromolecule may be obtained by exclusive reaction of the propagating groups, A*, as shown by the GTP of 2-(isobutyryl)ethyl methacrylate **(3)**.[22,23] The second linear analogue is made of L_C units (exclusive reaction of the initiating groups, B*) and leads to a polycondensate-type structure.

In this paper we describe the results of the self-condensing group transfer polymerization of MTSHEMA **(1)** under various reaction conditions. In particular, we investigate the influence of the GTP catalyst's type and of the reaction temperature on the reactivity ratio of the functional groups. This ratio, $r = k_A/k_B$, and the degree of branching, *DB*, are determined by quantitative ^{13}C NMR spectroscopy. We demonstrate that the self-condensing group transfer polymerization using slow monomer addition of MTSHEMA **(1)** to the monofunctional initiator 1-methoxy-3-(trimethylsilyloxy)-2-methyl-1-propene **(2)** (MTS, cf. Chart 1) can be employed to obtain hyperbranched methacrylates with a lower polydispersity. Finally, we show that the addition of methyl methacrylate (MMA) to living PMTSHEMA **(poly-1)** leads to star branched PMMA with a hyperbranched core ("hyperstar polymer").[13,19]

Experimental Section

NMR Spectra. ^{13}C NMR spectra were recorded at 100 MHz in $CDCl_3$ on a Bruker AM-400 spectrometer using the triplet peak of the solvent signal (δ = 77.0 ppm) as an internal standard. Inverse-gated decoupling (INGATED) ^{13}C spectra were recorded at room temperature on a Bruker DRX400 spectrometer at 100.6 MHz in $CDCl_3$. Numbers in the various spectra refer to the chemical structure depicted in Figure 5.

Reagents. Tetrahydrofuran (THF, BASF GmbH, 99.5+%) was distilled over a 1 m column and dried over potassium. After degassing, the solvent was stirred over sodium/potassium alloy and distilled in vacuo prior to use. Methyl methacrylate (MMA, BASF, 99.5+%) was distilled over a 1 m column filled with Sulzer packing at 45 mbar. After degassing, the distillate was stirred over CaH_2 (Aldrich, 99.99%), degassed, and distilled in high vacuum. 1-Methoxy-3-(trimethylsilyloxy)-2-methyl-1-propene **(2)** (MTS, ABCR, 99.9+%) was distilled under reduced pressure using a split-tube column and stored under high vacuum. Acetic acid (96 wt %, Acros, p.a.), methanol (BASF, 99+%), and tetrabutylammonium fluoride (1 M solution in THF, Aldrich) were used without prior purification. The GTP catalysts tetrabutylammonium bibenzoate[33] (TBABB), tetrabutylammonium bi(3-chlorobenzoate) [33](TBAB3ClB), tris-dimethylaminosulfonium bifluoride[34] ($TASHF_2$), the inimer 2-(2-methyl-1-triethylsiloxy-1-propenyloxy)ethyl methacrylate[22,23] (MTSHEMA) **(1)** and its vinyl analogue (2-(isobutyryl) ethyl methacrylate[22,23,35] **(3)**, and the corresponding linear polymer poly(2-(isobutyryl) ethyl methacrylate) **(poly-3)** were prepared according to known procedures. ^{13}C NMR (100 MHz) (2-(isobutyryl) ethyl methacrylate **(3)** δ/ppm: 167.05 (7); 136.04

Scheme 2. Linear Analogues of PMTSHEMA (Poly-1): (a) Vinyl-Type Polymer Poly(2-(isobutyryl)ethyl methacrylate) (Poly-3) Consisting of L_V Units and (b) Polyester-Type Polymer Composed of L_C Units

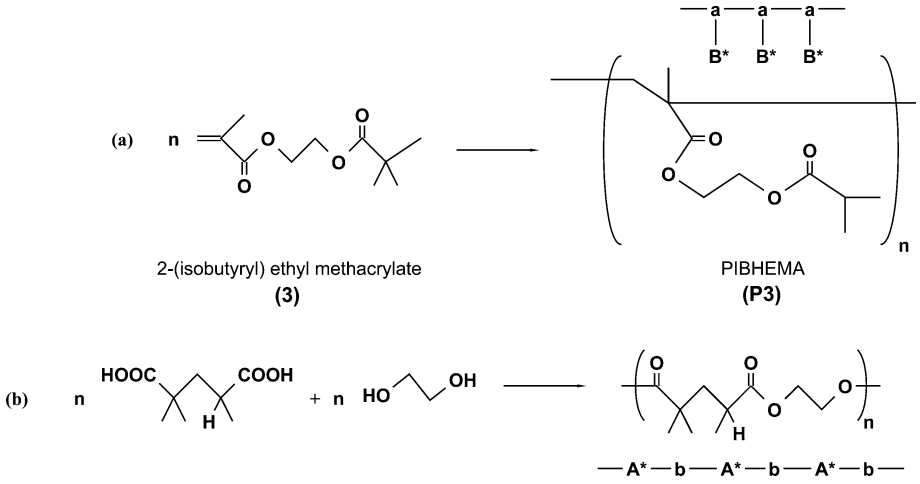

(6); 125.81 (5); 62.85 and 61.48 (4 and 4′); 33.77 (3); 18.84 (2); 18.21 (1). **(poly-3)** δ/ppm: 177.15 (7, mrrr and 8); 176.15 (7, rrrr); 175.94 (7, rmrr); 62.85 and 61.48 (6 and 6′ used for normalization in INGATED measurements), 54.33 (5); 45.01 (4, a group, mr); 44.72 (4, a group, rr); 33.77 (3 ≡ B* group) 20.64 (1, rmmr); 18.84 (1, rmrr, and 2); 16.65 (1, mrrm, mrrr, and rrrr). 2,2,4-Trimethyl glutaric acid dimethyl ester **(4)** and the cyclic trimer of MMA 2,4-(dicarbomethoxy)-2,4,6,6-tetramethylcylcohexanone **(5)** were kindly supplied by Dr. L. Lochmann, Prague.[36−39] ^{13}C NMR (100 MHz): 2,4-trimethylglutaric acid dimethyl ester **(4)** δ/ppm: 177.68 (9); 177.07 (8); 51.40 (7 and 7′); 43.86 (6); 41.77(5); 36.30 (4 ≡ A* group); 25.71 and 24.61 (2 and 3 ≡ b group); 19.14 (1 ≡ A* group); 2,4-(dicarbomethoxy)-2,4,6,6-tetramethylcylcohexanone **(5)** δ/ppm: 212.84 (14); 178.59 (13); 173.74 (12); 53.57 (11); 52.20 (10 and 9); 44.17 (8), 43.33 (7 ≡ C group); 39.88 (6 ≡ a_{CYC} goup); 39.36 (5); 29.37 (4); 27.82 (3); 25.89 (2); 22.76 (1).

Conversion Detection. The conversion of the inimer MTSHEMA **(1)** was monitored by gas chromatography using octane as internal standard. Samples of 10 μL were injected at a temperature of 120 °C on a Fisons GC 8000 system. A Megabore methylpolysiloxane capillary column DB1 (length: 30 m, 0.53 mm i.d., film thickness 1.5 μm) was employed as stationary phase and hydrogen as mobile phase. Separation was performed following a temperature ramp (50 °C for 4 min, then heating to 150 °C at a rate of 20 °C/min and keeping the temperature for additional 5 min). The components were detected with an FID operating at 170 °C. Raw data were recorded and evaluated using the ChromCard for Windows Software V1.17β.

Homopolymerization of MTSHEMA. All kinetic experiments were performed in a stirred tank reactor under a nitrogen atmosphere in THF. Adding the catalyst to the reaction mixture initiated the polymerization. Polymerizations were performed at different temperatures, varying the absolute concentration of the inimer MTSHEMA **(1)** and the type and concentration of the catalyst. In a typical experiment, the polymerization was initiated by the addition of 0.25 mL of the catalyst solution in THF ($C_0 = 1.67 \times 10^{-3}$ mol L^{-1}) to a mixture of 1 g of MTSHEMA **(1)** ($I_0 = 0.167$ mol L^{-1}) and 19 mL of THF. The polymerization was quenched with few drops of a methanol/acetic acid/tetrabutylammonium fluoride mixture (9:1:1). After evaporation of the solvent, the hyperbranched polymer **(poly-1)** was dissolved in benzene, filtered, and freeze-dried. The inimer and catalyst concentrations, reaction temperatures, and reaction times for all kinetic runs are provided in Table 2.

Semibatch Homopolymerization of MTSHEMA in the Presence of Initiator. A mixture of 1 g of MTSHEMA **(1)** (3.18 mmol) in 40 mL of THF and 61 mL of a solution of trisdimethylaminosulfonium bifluoride in THF ($c = 1.15 \times 10^{-5}$ mol/L; 6.97×10^{-4} mmol) were added separately but simultaneously under vigorous stirring over 165 min at a temperature of −20 °C to a solution of 0.012 g (0.0691 mmol) of MTS **(2)** in 10 mL of THF. Full conversion was reached after an additional 20 min. The polymerization was quenched with few drops of a methanol/acetic acid mixture (9:1). After evaporation of the solvent, the polymer **(poly-2)** was dissolved in benzene, filtered, and freeze-dried.

Preparation of Hyperstar PMMA. Polymerization of the hyperbranched precursor was achieved by adding 3.8 mL (1.99×10^{-3} mmol) of a tetrabutylammonium bi(3-chlorobenzoate) solution in THF (1.99×10^{-3} mmol) to 0.82 g of MTSHEMA **(1)** (2.59 mmol) in 15 mL of THF. After 20 min, 2 g of MMA (20 mmol) was added under vigorous stirring. Full conversion of MMA was reached after an additional 20 min. The polymerization was quenched with a few drops of a methanol/acetic acid/tetrabutylammonium fluoride mixture (9:1:1). After evaporation of the solvent, the hyperstar polymer was dissolved in benzene, filtered, and freeze-dried.

SEC Characterization. SEC measurements were performed at room temperature in THF using 5μ PSS SDV gel columns (10^3, 10^5, 10^6 Å, 30 cm each, column set 1; 10^3 Å (30 cm) and two 10^2 Å (60 cm each), column set 2; PSS GmbH, Mainz, Germany) at a flow rate of 0.5 mL/min. A Viscotek viscosity detector H 502B (operating at 30 °C), a Shodex RI-71 refractive index detector, and an Applied Biosystems 1000S UV diode array detector were used. Raw data were processed using PSS WinGPC V4.02 software. Universal calibration curves[40−42] $[\eta]M = f(V_e)$ were constructed using narrow PMMA standards in THF. Since this universal calibration curve is valid for any polymer structure, absolute molecular weights can be determined within an error range of 10%. Because of a low signal-to-noise ratio of the viscosity signal in the case of broadly distributed samples, a linear calibration curve based on PIBHEMA **(poly-3)** was used for polymers with $M_n < 2000$. In this molecular weight region, the effect of branching on the elution volume is not so much emphasized; consequently, the error range in the molecular weights is estimated not to exceed 10% (double-checked by universal calibration of a hyperbranched sample, which was fractionated by preparative SEC prior to the measurement).

Results and Discussion

Kinetics. Theoretical studies assuming equal reactivity of the different active groups ($k_A = k_B = k_p$) predict a quasi-first-order relation between the conversion of the inimer, x_I, and the reaction time, t. With the concentration of active groups, P^*, we obtain for the SCVP[43]

$$-\ln(1 - x_I) = k_p P^* t + 1 - e^{-kP^*t} = k_{app} t + 1 - e^{-k_{app}t} \quad (1)$$

Table 2. Experimental Conditions and Kinetic Results of the SCGTP of MTSHEMA (1) in THF

symbol	catalyst	I_0/mol L^{-1}	C_0/mol L^{-1}	T/°C	k_{app}/s^{-1}	$k_{p,app}$/L^2 mol^{-2} s^{-1}	t/min	x_I	M_n	M_w	M_w/M_n
⊡	TBAB3ClB	0.167	1.67×10^{-3}	20	7.6×10^{-3}	27.19	1	0.64	438	812	1.85
							4	0.92	691	1678	2.43
							16	1	935	2015	2.16
							32	1	775	1893	2.44
							64	1	760	1740	2.29
							128	1	676	1538	2.28
△	TBAB3ClB	0.167	1.67×10^{-3}	−20	1.5×10^{-4}	0.54	1	0.06	364	410	1.13
							4	0.05	380	425	1.12
							16	0.19	343	520	1.52
							32	0.62	871	1820	2.09
							64	0.86	1208	6620	5.48
▽	TBAB3ClB	0.167	1.67×10^{-3}	−40	6.8×10^{-6}	0.02	4	0.01	213	236	1.11
							16	0.02	218	247	1.13
							64	0.03	245	320	1.31
							128	0.11	255	339	1.33
							256	0.21	260	395	1.52
◇	TBAB3ClB	0.167	1.67×10^{-3}	0	1.8×10^{-3}	3.89	1	0.38	743	1834	2.47
							4	0.45	761	2506	3.29
							16	0.80	827	1970	2.38
							32	0.95	840	1780	2.12
							64	1	864	1660	1.92
							128	1	953	2236	2.35
■	TBABB	0.142	5.46×10^{-5}	−20	1.3×10^{-3}	103.10	2	0.40	830	1600	5.45
							8	0.78	1200	2300	6.21
							16	0.89	2250	12100	3.49
							32	0.94	2400	10500	4.17
							64	0.97	2450	13350	4.66
▼	TBABB	0.146	4.29×10^{-5}	0	3.8×10^{-3}	610.68	2	0.81	2100	13040	3.21
							4	0.79	4300	15000	3.49
							8	0.87	3800	15850	4.17
							16	0.99	3500	16300	4.66
							32	1	4800	15400	3.21
							64	1	10600	37700	3.56

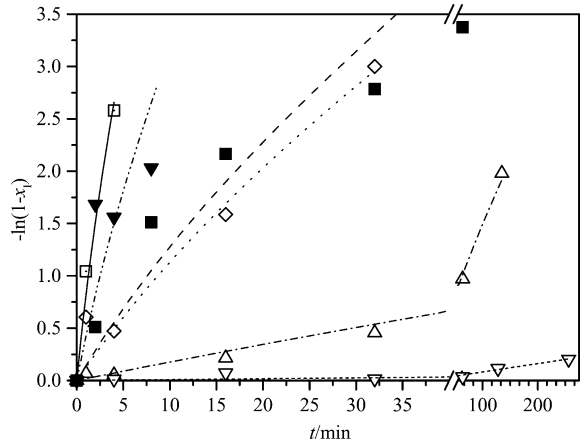

Figure 1. First-order time−conversion plots of the SCGTP of MTSHEMA (**1**) varying the reaction conditions. Reaction conditions and symbols are explained in Table 2. The fit curves were obtained by nonlinear curve fit according to eq 1 assuming equal reactivity of active groups ($k_A = k_B = k$).

From a nonlinear curve fit of the dependence of the conversion of inimer on time according to eq 1, only an apparent rate constant, $k_{app} = k_p P^*$, can be determined. In the limiting cases

$$\text{for } k_{app}t \ll 1: \; -\ln(1 - x_I) = k_{app}t \tag{2}$$

$$\text{for } k_{app}t \gg 1: \; -\ln(1 - x_I) = 2k_{app}t \tag{3}$$

a linear dependence of the conversion, x_I, with the time is yielded. The first-order time−conversion plots of the homopolymerization of the inimer MTSHEMA **(1)** under different reaction conditions (cf. Table 2) are outlined in Figure 1. From these dependences the apparent rate constant, k_{app}, was determined by a nonlinear curve fit according to eq 1. The corresponding fit curves are also

Scheme 3. Kinetic Scheme for Group Transfer Polymerization

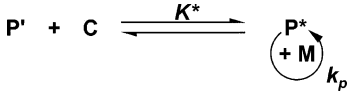

depicted in Figure 1; the apparent rate constants, k_{app}, can be found in Table 2.

To determine the "true" rate constant, k_p, the explicit knowledge of the concentration of active groups, P^*, is necessary. However, P^* cannot be obtained experimentally because of a dynamic equilibrium between dormant chain ends, **P′**, and the catalyst, **C**, on the left-hand side and active chain ends, **P***, on the right-hand side in Scheme 3.[44]

The position at the equilibrium is governed by the equilibrium constant, K^*. Use of the mass action law renders under the assumption $C_0 \ll I_0$ and $P^* \ll I_0$ for the concentration of active species

$$P^* = \frac{K^* I_0}{1 + K^* I_0} C_0 \tag{4}$$

It is obvious that for $K^* I_0 \gg 1$ the equilibrium is shifted to the right-hand side, i.e., $P^* = C_0$, whereas for $K^* I_0 \ll 1$ ($P^* = K^* I_0 C_0$) the dormant species is the preferred one. In the present case the equilibrium constant, K^*, is not known explicitly. However, from earlier kinetic investigations[44] it is known that for oxyanion catalysts, such as the ones used here, the latter case is valid. Hence, we define a "pseudo" rate constant, $k_{p,app}$

$$k_{p,app} = \frac{k_{app}}{C_0 I_0} = k_p K^* \tag{5}$$

which is experimentally accessible.

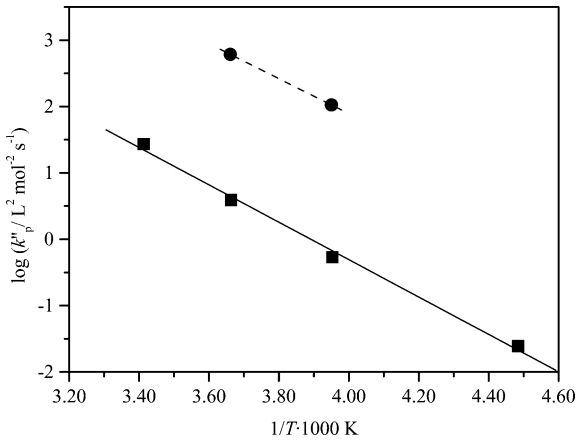

Figure 2. Arrhenius plot of the "pseudo" rate constants, $k_{p,app} = k_{app}/(C_0I_0)$. Symbols and results of the linear fit are given in Table 3.

Table 3. Apparent Activation Energies, $E_{a,app}$, and the Apparent Frequency Exponents, log A_{app}, for the SCGTP of MTSHEMA (1) for Various Catalysts

catalyst	symbol in Figure 2	$E_{a,app}$/kJ mol^{-1}	log A_{app}
TBABB[a]	●	58.1	14.1
TBAB3ClB[b]	■	54.1 ± 2.5	11.0 ± 0.5

[a] Tetrabutylammonium bibenzoate. [b] Tetrabutylammonium bi(3-chlorobenzoate).

The dependence of the pseudo rate constants, $k_{p,app} = k_{app}/(C_0I_0)$, on temperature for TBABB and TBAB3ClB catalysts is depicted in Figure 2. A linear fit of the data in the Arrhenius plot (Figure 2) yields the apparent activation energy, $E_{a,app}$, and the apparent frequency exponent, log A_{app} (cf. Table 3).

Within the experimental error, the apparent activation energies, $E_{a,app}$, for the different catalysts are similar. The apparent preexponential factors, log A_{app}, however, differ between TABB and TBA3ClB in 3 orders of magnitude. As the apparent activation parameters are linked to the "real" ones via the enthalpy, ΔH^*, and entropy, ΔS^*, of the activation equilibrium

$$E_{a,app} = E_a + \Delta H^* \tag{6}$$

and

$$\log A_{app} = \log A + \frac{\Delta S^*}{R} \tag{7}$$

the different reaction rates (cf. Figure 1) are due to a higher activation entropy (lower frequency exponent A). It can be concluded that in the case of TBAB3ClB this equilibrium is more shifted toward the dormant species as compared to the TBABB catalyst. This is explained by the lower nucleophilicity of the bi(3-chlorobenzoate) anion relative to the bibenzoate one.

Dependence of Molecular Weight Distribution on Conversion. The dependence of the molecular weight distribution on the conversion of MTSHEMA **(1)**, x_I, for a batch polymerization was monitored by varying the absolute concentrations of the inimer, I_0, as well as the type and concentrations of catalyst, C_0 (cf. Table 2). The results are depicted in parts a and b of Figure 3, respectively.

A comparison with the theoretical predictions is not straightforward as the theory of the SCVP kinetics was developed using the conversion of all *vinyl* groups, x, i.e., all of the inimer's *and* the macromolecule's ones.

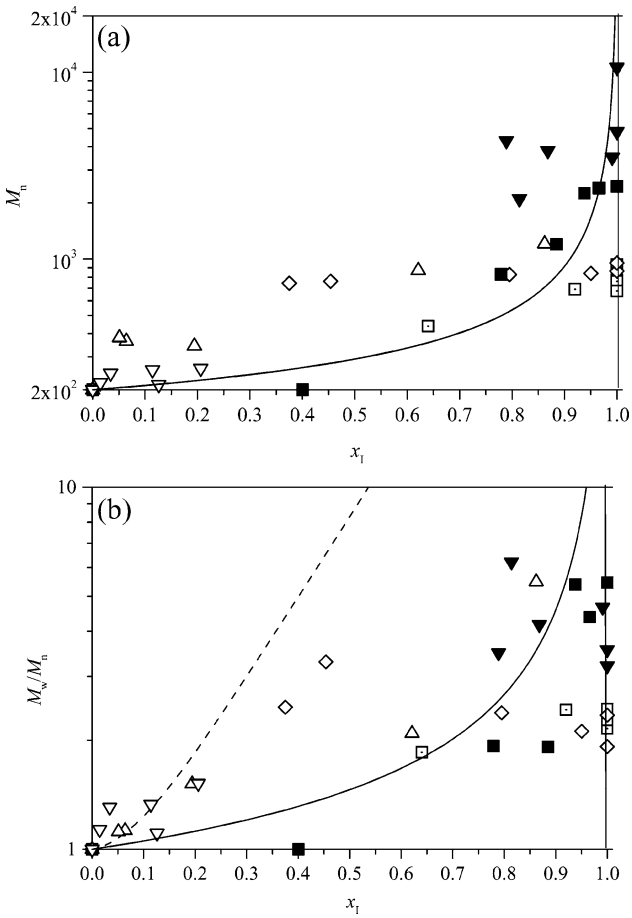

Figure 3. Plot of the number-average molecular weight (a) and the polydispersity index (b) vs the conversion of inimer, x_I, for the SCGTP of MTSHEMA (**1**). Symbols see Table 2. For comparison results according to the SCVP theory for a ratio $r = 1$ (—) and $r = 100$ (- - -) are also shown. The results were computed according to Figures A3-1 and A4-1 of the Supporting Information of ref 11.

The two conversions, x_I and x, are related, assuming the different rate constants k_A and k_B are independent of the degree of polymerization.[43] This assumption, however, does not necessarily require equal rate constants; hence, eq 8 can also be employed in the case $r = k_A/k_B \neq 1$. The relation reads

$$x_I = 1 - (1 - x)e^{-x} \tag{8}$$

In the case of equal rate constants, $r = 1$, the dependence of the number-average degree of polymerization, P_n, can be expressed as

$$P_n = \frac{P_w}{P_n} = \frac{1}{1 - x} \tag{9}$$

Both expressions are plotted in Figure 3a,b as a function of the conversion of inimer, x_I, by altering x into x_I using eq 8.

In the case of unequal reactivities of initiating B* and propagating A* groups the complete molecular weight distribution cannot be calculated analytically. However, the expression for the number-average degree of polymerization, P_n, is unchanged and independent of the reactivity ratio $r = k_A/k_B$.[11] Any other average of the degree of polymerization or molecular weight has to be determined numerically. Because the reactivity ratio of

Scheme 4. Example for the "Backbiting" Reaction in the GTP of MTSHEMA (1); Functional Groups and Chemical Structure of the Reaction Are Shown

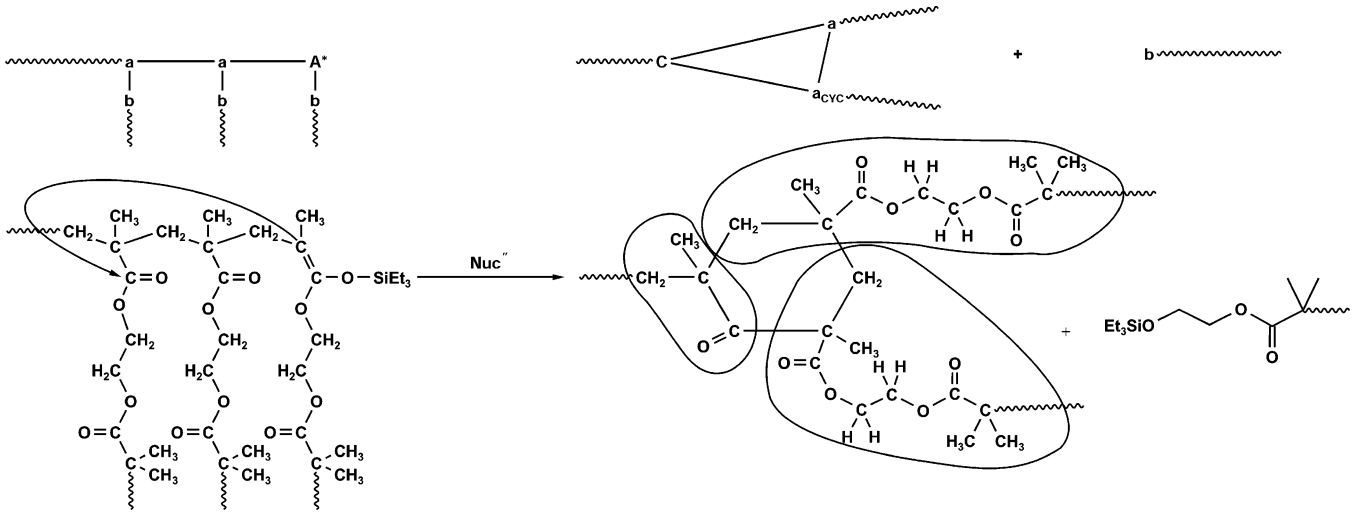

the MTSHEMA system was found to be in the range $10 < r < 40$ (vide infra), the theoretical dependence of the number-average degree of polymerization and the polydispersity as a function of the conversion of inimer, x_I, for $r = 1$ and $r = 100$ are also shown in Figure 3a,b. For low conversions, the experimental values for the M_n and the M_w/M_n generally correspond to the theoretical predictions. For conversions $x_I \geq 0.9$, however, the experimental data are always below the theoretical ones.

The reactivity ratio $r = k_A/k_B$ is known to influence the molecular weight distribution. As indicated in Figure 3a,b the case $r > 1$ leads to an increase of the polydispersity index, making the discrepancy between theory and experiment even larger. Possible reactions which can explain this difference are (i) the backbiting reaction[45] and (ii) the cyclization reaction.[26,28]

In the case of a backbiting reaction,[45] the nucleophilic group of an active chain end attacks a penultimate carbonyl group. A cyclic β-keto ester is formed which contains two new types of functional groups, a_{cyc} and C, respectively. Unlike backbiting in a linear polymer, in the case of a hyperbranched ones whole branches of the macromolecule will be detached resulting in a lower degree of polymerization[22] (cf. Scheme 4).

Backbiting products can be identified by SEC−UV coupling methods, as the resulting β-keto ester possesses an absorption maximum at $\lambda \approx 300$ nm (as detected from the cyclic trimer **(5)**).[45] In an SEC analysis the RI signal is proportional to the polymer's *weight*, whereas the UV($\lambda = 300$ nm) signal corresponds to the *number* of β-keto ester units in the macromolecule. Consequently, the amount of backbiting can be judged from ratio of the molar mass-weighted UV($\lambda = 300$ nm) and the RI signal, UV($\lambda = 300$ nm)·M/RI. In Figure 4 two eluograms for reaction times of 1 and 135 min are compared. For short reaction times, no UV($\lambda = 300$ nm) signal is detected, demonstrating the absence of backbiting. After 135 min the ratio $UV(\lambda = 300\text{ nm})\cdot M/RI$ increases dramatically, especially for low elution volumes, V_e, indicating the occurrence of multiple backbiting reactions per polymer.

In the cyclization reaction an active group of a hyperbranched macromolecule reacts intramolecularly with the double bond. A multifunctional macroinitiator containing one loop is yielded, which lacks the double

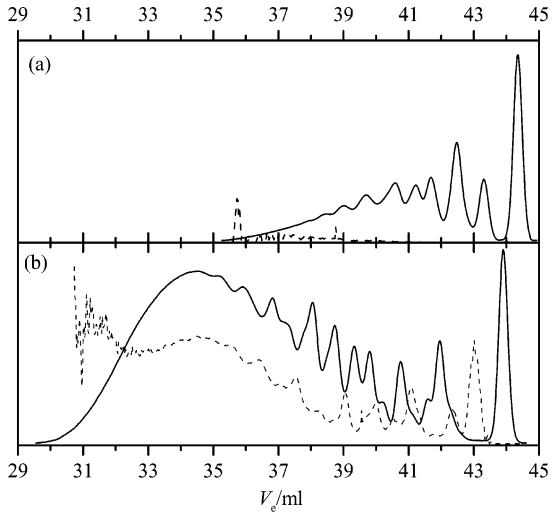

Figure 4. SEC traces at reaction times (a) 1 min and (b) 135 min of a SCGTP of MTSHEMA. Reaction conditions: $I_0 = 0.167$ mol/L, $C_0 = 3.34 \times 10^{-4}$ mol/L, TBAB3ClB. (—): RI signal, (- - -): UV($\lambda = 300$ nm)·M/RI. Column set 2.

bond. In consequence, the reaction kinetics are altered. This effect was studied theoretically for AB_2 polycondensation using Monte Carlo simulation.[26,28] The results of the simulation predict the fraction of cyclic x-mers to increase with increasing degree of polymerization, P_n, and overall conversion. Consequently, the polydispersity will decrease,[29,30,46] and the number as well as the weight-average molecular weights do not diverge but remain finite even at complete conversion of the vinyl groups.[26,27]

According to Figure 3a, the increase of the molecular weights with conversion of vinyl groups, x, is slower than predicted for a SCVP, especially at high conversions. It may be hypothesized that this finding is attributed to the backbiting reaction. As vinyl groups are not affected in this reaction, backbiting cannot influence the conversion of vinyl groups at all. Moreover, the strong derivation in the kinetics of the SCGTP of MTSHEMA **(1)** from theoretical predictions, especially the occurrence of finite molecular weights at complete conversion of vinyl groups are indicating the presence of the cyclization reaction. It has to be stressed that this is only an indirect indication for the occurrence of cyclization. As the molecular structures of a hyper-

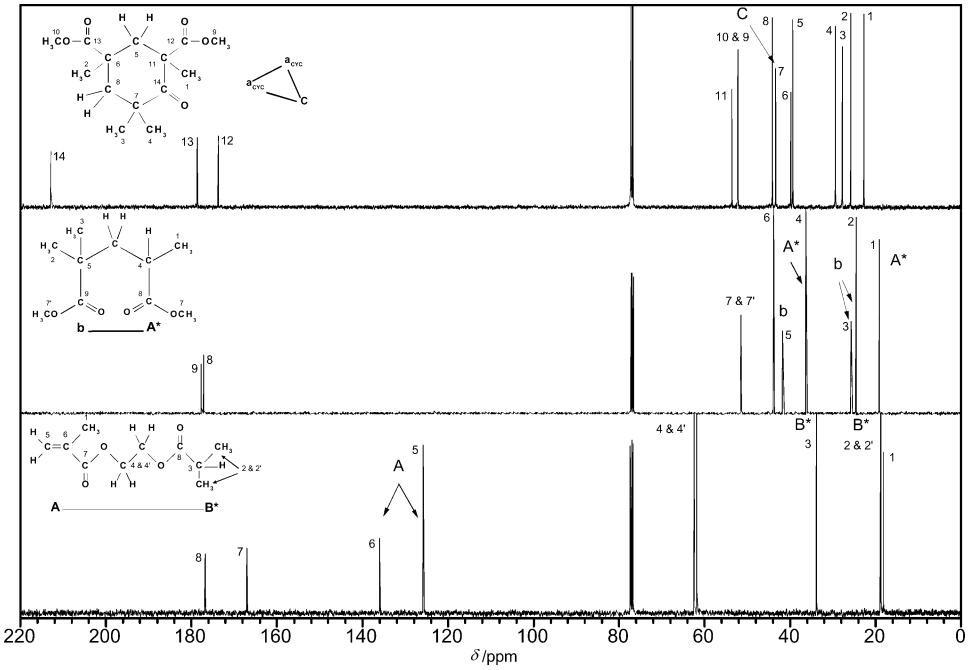

Figure 5. 100 MHz ^{13}C NMR spectra of the model compounds 2,4-(dicarbomethoxy)-2,4,6,6-tetramethylcylcohexanone (**5**) (upper part), 2,2,4-trimethylglutaric acid dimethyl ester (**4**) (middle part), and (isobutyryl)ethyl methacrylate (**3**) (lower part). The numbers refer to the chemical shifts given in the experimental part, and the letters represent the different functional groups.

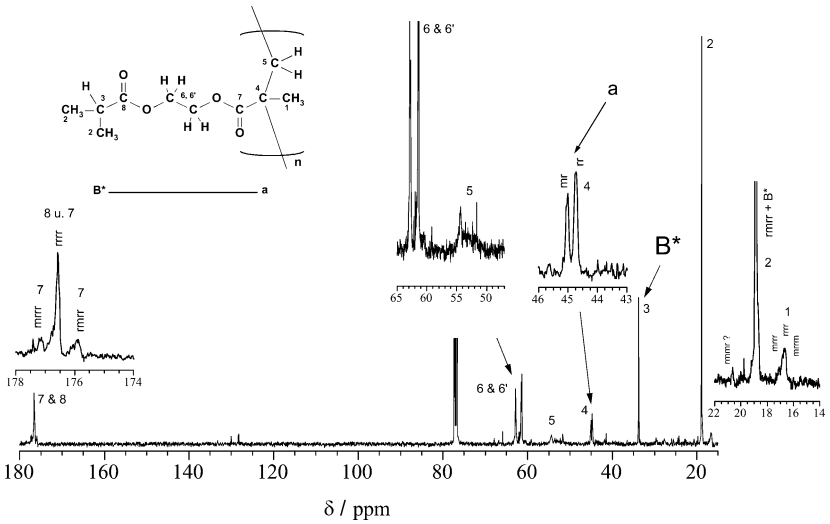

Figure 6. 100 MHz ^{13}C NMR spectra of the linear model polymer poly(2-(isobutyryl)ethyl methacrylate) **(poly-3)**. Numbers refer to the chemical shifts given in the experimental part, and the letters represent different functional groups.

branched polymer in the presence and the absence of cyclization only differ in the structure of *one* single group per macromolecule direct determination of cyclization can only be accomplished using advanced mass spectroscopy methods as pointed out by Dušek et al.[26]

Determination of the Degree of Branching. a. Model Compounds. To estimate the shifts of the different groups present in hyperbranched polymers model compounds were analyzed by ^{13}C NMR. In the case of **(poly-1)** the structural motif of the a- and B*-moieties can be found in the linear polymer poly(2-(isobutyryl) ethyl methacrylate) **(poly-3)**. The chemical environment of the A*-group is mimicked in 2,2,4-trimethylglutaric acid dimethyl ester **(4)**. A pattern similar to the C- and a_{cyc}-moieties can be found in 2,4-(dicarbomethoxy)-2,4,6,6-tetramethylcylcohexanone **(5)**, the cyclic trimer of MMA. The corresponding ^{13}C NMR spectra of model compounds **3**−**5** are depicted in Figure 5, whereas the spectrum of **(poly-3)** is shown in Figure 6.

Hence, six different functional groups have to be considered for the calculation of the degree of branching, *DB*: The tertiary carbon atom of the initiating moiety, B*, is substituted with two methyl groups and one carbonyl group. The tertiary carbon atom of the propagating moiety, A*, is surrounded by a methylene group of the main chain, a carbonyl group, and only one methyl group, resulting in a slightly different chemical shift compared to the B*. A similar motif is found for the quaternary a- and b- moieties, in which the methylene group of the polymer chain replaces the proton of the active groups. The presence of a β-keto ester group stemming from the backbiting reaction results in two additional moieties to be considered. In the β-group the quaternary carbon is attached to the keto group and consequently differs in its chemical environment from all the patterns discussed above. Furthermore, the different chemical environment due to the neighborhood to a β-keto ester results in a

Table 4. Functional Groups in SCGTP of MTSHEMA (1)

unit	δ / ppm	structure (quenched)[a]	unit	δ / ppm	structure[a]
A*	19,5 and 36,4	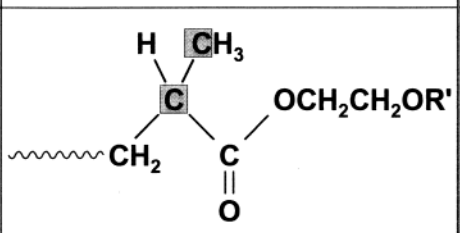	a	46,0 to 45,0	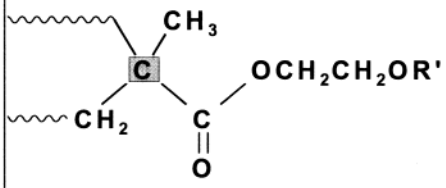
B*	34,0	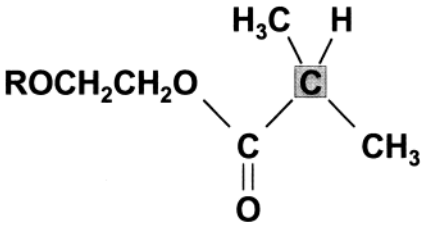	b	25,2	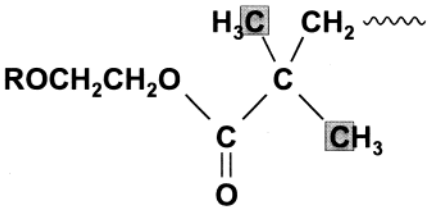
C	43,3	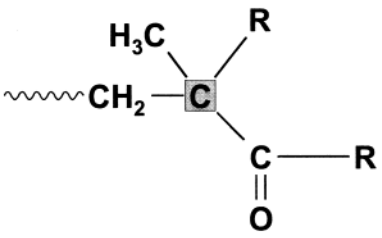	a_{CYC}	40,2	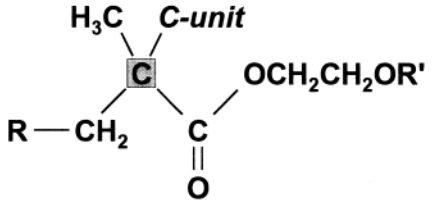

[a] Carbon atoms used for determination of the group's fractions in ^{13}C NMR are shaded. Curved lines represent parts of the molecule that are connected to polymer chains. R′ represents the B* or b part of an MTSHEMA (**1**) molecule or polymer, and R represents the A*, a_{CYC}, or a part.

downfield shift of the adjacent a-group leading to a_{CYC}-moieties.

b. Evaluation of the Spectra. To determine the degree of branching, *DB*, experimentally polymer **(poly-1)** was analyzed by ^{13}C-INGATED-NMR spectroscopy. The different functional groups composing the hyperbranched polymer are depicted in Table 4 (see also Scheme 1 and Scheme 4), and a representative ^{13}C-INGATED spectrum is shown in Figure 7.

According to Yan[32] and Hölter,[47] the degree of branching, *DB*, reads in the general case (cf. Table 1)

$$DB = \frac{(\text{no. of branched units}) + (\text{no. of terminal units}) - 1}{(\text{total no. of units}) - 1} \quad (10)$$

In AB_2 or AB* systems with trifunctional branch points the number of branched units equals the number of terminal units minus one. Rewriting eq 10 results in

$$DB = \frac{2(\text{no. of branched units})}{2(\text{no. of branched units}) + (\text{no. of linear units})} \quad (11)$$

as the total number of units is the sum over branched, linear, and terminal ones. Rewriting (11) using the symbols introduced in Table 1 yields

$$DB = \frac{2D}{2D + L_V + L_C} \quad (12)$$

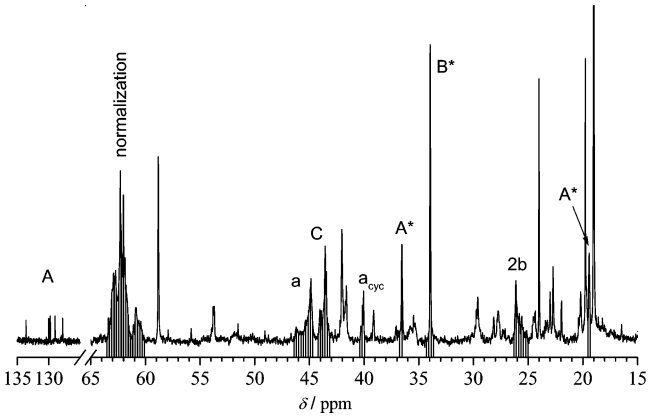

Figure 7. Representative 100 MHz ^{13}C-INGATED NMR-spectra of **poly-1**. Shaded areas were used to compute the degree of branching, DB_{NMR}.

However, from the ^{13}C spectrum the fraction of functional groups rather than the number of units can be detected. As pointed out by Yan,[32] the fractions of various structural units are identical to the products of the fractions of the active or reacted groups of which they consist of. During the backbiting reaction a_{cyc} and C groups are generated. The a_{cyc} group can be incorporated in D or L_C units. The C group has to be considered as a linear unit as the backbiting reaction does not create an additional branch point (cf. Scheme 4). Using the correlations given in Table 1, the calculation of the degree of branching, DB_{NMR}, from ^{13}C-INGATED NMR spectra can be accomplished. Finally, it reads

$$DB_{NMR} = \frac{2D}{2D + L_V + L_C + C} = \frac{2(a + a_{cyc})b}{2(a + a_{cyc})b + A^*b + (a + a_{cyc})B^* + C} \quad (13)$$

whereas the fraction of the various functional groups was obtained by normalization of their intensity in the spectrum with respect to the (−O−CH_2−CH_2−O−) group. The results are given in Table 5.

Using the relation between the various functional groups in a hyperbranched polymer for full conversion of double bonds and inimer, respectively[32]

$$a = B^* \quad \text{and} \quad b = 1 - B^* \quad (14)$$

and defining a ratio of reacted groups

$$\Xi = \frac{a + a_{cyc}}{b} \quad (15)$$

we obtain for the fraction of initiating groups

$$B^* = \frac{\Xi}{\Xi + 1} \quad (16)$$

In analogy to the results of Yan et al.[32]

$$r_{theo} = \frac{B^*}{B^* - \ln B^* - 1} \quad (17)$$

the reactivity ratio at full conversion as determined from the NMR spectra, r_{NMR}, can also be computed by the use of eqs 16 and 17

$$r_{NMR} = \frac{k_A}{k_B} = -\frac{\Xi}{1 + (1 + \Xi)\ln\left(\frac{\Xi}{1 + \Xi}\right)} \quad (18)$$

It has to be stressed that eq 17 was derived for ideal SCVP conditions, i.e., absence of backbiting and cyclization. In the "ideal" case, the degree of branching, DB_{theo}, could also be estimated from its dependence on the reactivity ratio, r_{theo}.[14,16,32] However, the occurrence of backbiting and cyclization reactions makes this procedure erroneous in the present case.

The dependence of the reactivity ratio, r_{NMR}, and the degree of branching, DB_{NMR}, on the reaction conditions of the self-condensing group transfer polymerization of MTSHEMA **(1)** are outlined in Table 5. Furthermore, the results of Sakamoto's et al. study[23] are included in that compilation using their ratio of reacted groups, Ξ, to calculate the corresponding r_{NMR} according to eq 18. Because of their lack of data on the fraction of structural units, we were not able to calculate the degree of branching using eq 13. To correlate their results with ours, we calculated a theoretical degree of branching, DB_{theo}, by neglecting the presence of backbiting (i.e., assuming $r_{NMR} = r_{theo}$) and using the theoretical dependence given in Figure 5 of ref 32.

According to Table 5, the degree of branching is strongly influenced by the type of catalyst used. However, our results are at variance with those of Sakamoto's group. Probably, these differences are due to the precipitation of their polymers, which excludes lower molecular weight compounds from analysis. The results of Table 5 indicate that the activation equilibrium is shifted more to the deactivated species. The effect is especially prominent in the case of oxyanion-type catalysts, resulting in a lower reaction rate compared to that of the fluoride-type catalysts. These differences in the "silicophilicity" of the catalyst system also influence the reactivity ratio, r, and the degree of branching, DB. It seems that in the case of the less "silicophilic" oxyanions the deactivation process of the propagating groups, A*, is not fast enough, and vinyl addition can occurs several times before the deactivation takes place. In the case in the more "silicophilic" fluoride catalyst, the deactivation process occurs faster, leading to lower reactivity ratios and a higher degree of branching.

Table 5. Dependence of the Reactivity Ratio, $r_{NMR} = k_A/k_B$, and the Degree of Branching, DB_{NMR}, on the Reaction Conditions for the SCGTP of MTSHEMA (1)

catalyst	T/°C	Ξ	DB_{NMR}[b]	r_{NMR}	DB_{theo}[c]
TBAB3ClB	−20	3.1	0.24	22.7	0.36
TBAB3ClB	0	3.0	0.38	19.4	0.38
TBABB[a]	20	2.1		10.1	0.43
TASHF2	−20	2.4	0.42	13.4	0.41
TASHF2	0	2.2	0.25	13.1	0.42
$TASHF_2$[a]	20	4.2		38.1	0.31

[a] Results of Sakamoto et al.[23] [b] Calculated using eq 13. [c] Obtained from the theoretical dependence $DB = f(r)$ according to Figure 5 of ref 32.

Another explanation may be found in a direct exchange of activities between living and dormant chain ends. This degenerative transfer is a well-known feature of the GTP.[48] Especially in the case of oxyanion catalysis this effect is known to influence the molecular weight distribution as well as the reaction kinetics. Hence, it is very likely that this effect may account for the "slower" deactivation process of the A* groups.

Similar reactivity ratios were reported other SCVP systems. Matyjaszewski et al.[16] found reactivity ratios $r \approx 4.3$ for the ATRP of 2-(2-bromopropionyloxy)ethyl acrylate, whereas Weimer et al.[14] reported reactivity ratios spanning from $12 \leq r \leq 34$ for the ATRP of 4-(chloromethyl)styrene. Consequently, the higher apparent reactivity of the propagating groups appears to be a general feature of the SCVP.

Semibatch Polymerization of MTSHEMA in the Presence of Initiator. Theoretical calculations predict that SCVP using slow inimer addition to an f-functional initiator leads to a decrease of polydispersity[30,46]

$$\frac{M_w}{M_n} \approx 1 + \frac{1}{f} \quad (19)$$

In contrast to the batch process, P_n is determined by the ratio of inimer to initiator, I_0/G_0. Figure 8 shows an SEC trace of the hyperbranched polymer **(poly-2)** (cf. Table 6 for MWD) which was prepared by slow addition of MTSHEMA **(1)** to the monofunctional initiator MTS **(2)**. Since the rate of inimer addition cannot be infinitesimally low, inimer molecules may not exclusively add to initiator molecules or to MTS initiated macromolecules. The addition to other inimer molecules leads to MTSEHEMA homopolymers **(poly-1)** with vinyl groups, which serve as initiators themselves. The coexistence of two different types of propagating macromolecules eventually leads to a broadened bimodal MWD.[30,46]

Assuming equal rate constants of A* and B* groups, the z-distribution of a semibatch SCVP in the presence

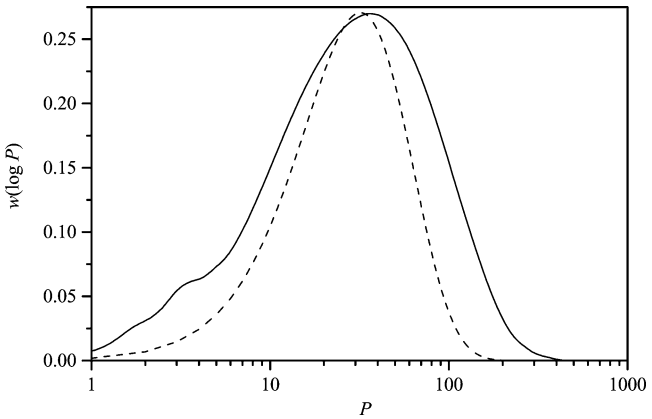

Figure 8. Comparison of the *z*-distributions of **(poly-2)**(—) and the *z*-distribution predicted by theory for a $P_n = 16$ (- - -).

Table 6. Molecular Weight Averages and Degree of Branching, DB_{NMR}, in the SCGTP of MTSHEMA (1) for Semibatch and Batch Experiments in the Presence of Monofunctional Initiator MTS (2)

	I_0/G_0	P_n	P_w/P_n	DB_{NMR}
semibatch	46	16	2.8	0.42
batch run[a]		14	2.7	0.44

[a] In the absence on an initiator.

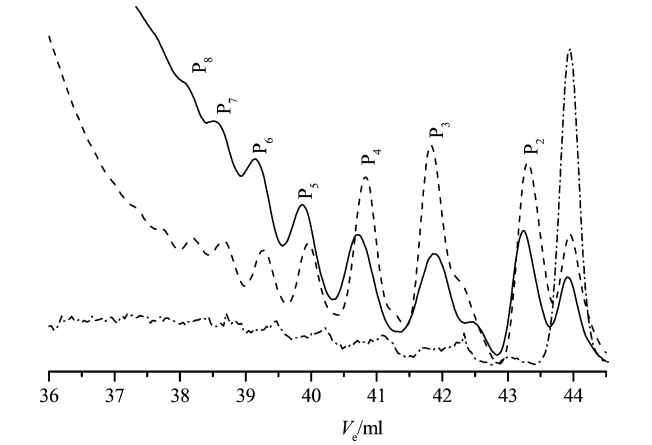

Figure 9. Blowup of the SEC traces (oligomeric region) of hyperbranched **(poly-2)** and linear **(poly-3)** polymer: (—) RI signal of **(poly-2)**; (- · -) UV(λ = 300 nm)·M signal of **(poly-2)**; (- - -) RI signal of **(poly-3)**. Column set 2.

of a monofunctional initiator ($f = 1$) reads[30]

$$w(\log P) = z(P) = \frac{(P/P_n)^2 e^{-P/P_n}}{2} \qquad (20)$$

where P denotes the degree of polymerization. In Figure 8 the *z*-distribution calculated according to eq 20 for a number-average degree of polymerization of $P_n = 16$ is compared to the experimental results for **(poly-2)**. It is obvious from Figure 8 that **(poly-2)** exhibits a broader molecular weight distribution than predicted by theory. Further insight into the polymer's structure reveals Figure 9, where the SEC traces of the oligomeric region of the hyperbranched **(poly-2)** and the linear analogue **(poly-3)** are compared. In Figure 9 the assignment of signals to various degrees of polymerization, P, was performed by counting the number of peaks starting with the elution volume of 2-(isobutyryl)ethyl methacrylate **(3)** (protonated MTSHEMA **(1)**) at $V_e = 48.02$ mL. As shoulders of the peaks of P_2 and P_3, signals with

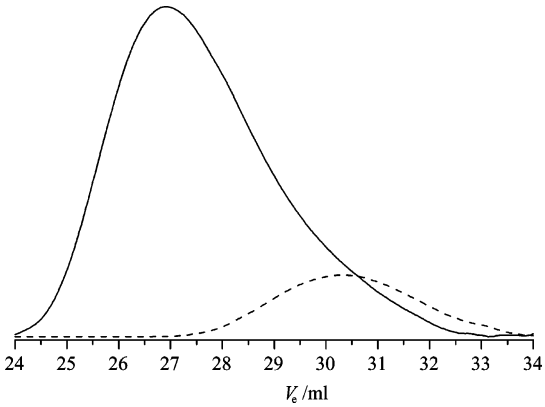

Figure 10. GPC traces (RI signal) of hyperstar polymer (—) and hyperbranched precursor (- - -). Molecular weight averages (universal calibration): hyperstar M_n = 10 300; D = 2.2; precursor M_n = 2000; D = 1.7. Column set 1.

low intensity are detected at elution volumes higher than the main peak. According to the absorption in the UV(λ = 300 nm) these signals can be identified as backbiting products, formed at the early stages of the polymerization. Unlike the results of a batch polymerization, no absorption in the UV(λ = 300 nm) could be detected for lower elution volumes, indicating the absence of backbiting in the case of higher molecular weight species. The good agreement in the peak maxima of the MTS initiated linear analogue **(poly-3)** and hyperbranched **(poly-2)** shows that the major part of the hyperbranched polymer was initiated by the monofunctional initiator MTS **(2)**, i.e., the concentration of **(poly-1)**-type macromolecules is low.

In Table 6 the results of a batch run and a semibatch polymerization of MTSHEMA **(1)** performed at corresponding conditions are compared. As the molecular weight distribution of the batch polymerization is governed by backbiting and cyclization (vide supra), both weight distributions appear to be similar.

The degree of branching, DB_{NMR}, of **(poly-2)** was calculated using ^{13}C-INGATED NMR. The results are given in Table 6. No significant differences between **(poly-1)** and **(poly-2)** can be found with respect to the degree of branching. From the theoretical considerations[30] a maximum degree of branching, $DB = {}^2/_3$, can be expected for infinitesimally slow addition of the inimer for equal reactivity of A* and B* groups ($r = 1$). As there are no theoretical treatments, how the reactive ratio and the addition of the inimer within a finite period will affect the degree of branching, it is hard to interpret those results.

Synthesis of Hyperstar PMMA. The use of living hyperbranched polymers as a multifunctional initiator was previously described by some authors.[13,19] The effect of the addition of MMA to a living **(poly-1)** precursor is demonstrated in Figure 10. The peak maximum of the resulting hyperstar molecule is shifted to lower elution volumes; consequently, its molecular weight averages (universal calibration, precursor M_n = 2000, i.e., $P_n = 10$ and $D = 1.7$; hyperstar M_n = 10 300 and D = 2.2) are significantly increased compared to that of the hyperbranched precursor. Since the number of active groups in SCVP equals P_n, the hyperstar polymer has an average of 10 arms with average arm length of $M_{n,arm} = 830$.

Absolute molecular weights of the hyperstar polymer were determined by universal calibration. From the

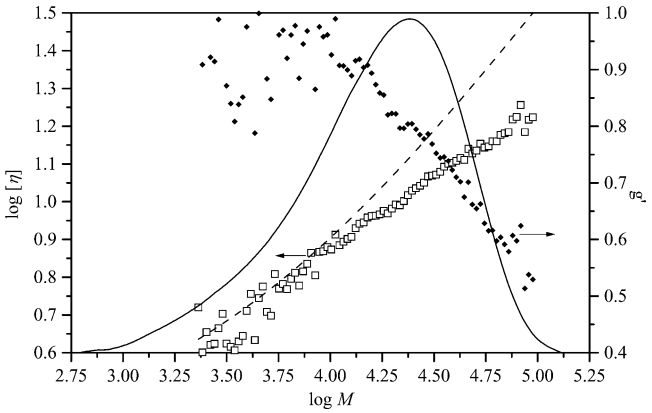

Figure 11. Mark−Houwink plot for hyperstar and linear PMMA. Key: intrinsic viscosity of hyperstar (□) and linear (- -) PMMA. (—): RI signal, (◆): contraction factors of hyperstar PMMA. The fit of the intrinsic viscosity of hyperstar PMMA yields a Mark−Houwink exponent of $\alpha = 0.37$.

measured viscosities and the absolute molecular weight distribution, Mark−Houwink plots were established (Figure 11). Contraction factors $g' = [\eta]_{br}/[\eta]_{lin}$ were calculated using viscosity data of linear PMMA for $[\eta]_{lin}$. The contraction factors decrease with increasing molecular weights showing a densely packed structure. Furthermore, the branched architecture is corroborated by the low Mark−Houwink exponent of $\alpha = 0.37$ (cf. $\alpha = 0.688$ for linear PMMA[49]).

Conclusion

The self-condensing group transfer polymerization of the inimer MTSHEMA **(1)** leads to hyperbranched polymethacrylates. However, molecular weights are lower and the molecular weight distribution is narrower than predicted from the theory of self-condensing vinyl polymerization. As judged from kinetic data and multidetector SEC results, cyclization and backbiting are responsible for this effect. The degree of branching, *DB*, and reactivity ratios of the two active groups, $r = k_A/k_B$, were determined by quantitative ^{13}C NMR spectroscopy. Reactivity ratios indicate a higher reactivity of the B* group, resulting in a $DB < 0.5$. A better reaction control is obtained by using slow addition of MTSHEMA **(1)** to the initiator MTS **(2)**. Furthermore, the addition of MMA to a living hyperbranched precursor yields a densely packed structure as revealed by the corresponding Mark−Houwink plots.

Acknowledgment. This work was supported by the Deutsche Forschungsgemeinschaft. P.S. thanks Peter Blumers, Mainz, for his helping hands in the laboratory. Finally, the authors are indebted to Dr. W. Radke, Darmstadt, for initializing their research activities on hyperbranched polymers.

References and Notes

(1) Flory, P. J. *Principles of Polymer Chemistry;* Cornell University Press: Ithaca, NY, 1953.
(2) Flory, P. J. *J. Am. Chem. Soc.* **1953**, *74*, 2718.
(3) Baker, A. S.; Walbridge, D. J. Imperial Chemical Industries Limited, London, England, US Patent 3,669,939; CA: 76: 128968h.
(4) Kim, Y. H.; Webster, O. W. *J. Am. Chem. Soc.* **1990**, *112*, 4592.
(5) Fréchet, J. M. J.; Hawker, C. J.; Lee, R. *J. Am. Chem. Soc.* **1991**, *113*, 4583.
(6) Mori, H.; Müller, A. H. E. In *Dendrimers V*; Schalley, C. A., Vögtle, F., Eds.; *Top. Curr. Chem.* **2003**, *228*, 1.
(7) Mori, H.; Müller, A. H. E. *Prog. Polym. Sci.* **2003**, *28*, 1403.
(8) Fréchet, J. M. J.; Henmi, M.; Gitsov, I.; Aoshima, S.; Leduc, M. R.; Grubbs, R. B. *Science* **1995**, *269*, 1080.
(9) Hazer, B. *Macromol. Rep.* **1991**, *A28 (Suppl. 1)*, 47.
(10) Hazer, B. *Makromol. Chem.* **1992**, *193*, 1081.
(11) Müller, A. H. E.; Yan, D.; Wulkow, M. *Macromolecules* **1997**, *30*, 7015.
(12) Puskas, J. E.; Grasmüller, M. *Macromol. Symp.* **1998**, *132*, 117.
(13) Gaynor, S. G.; Edelman, S.; Matyjaszewski, K. *Macromolecules* **1996**, *29*, 1079.
(14) Weimer, M. W.; Fréchet, J. M. J.; Gitsov, I. *J. Polym. Sci., Part A* **1998**, *36*, 955.
(15) Matyjaszewski, K.; Gaynor, S. G.; Kulfan, A.; Podwika, M. *Macromolecules* **1997**, *30*, 5192.
(16) Matyjaszewski, K.; Gaynor, S. C.; Müller, A. H. E. *Macromolecules* **1997**, *30*, 7034.
(17) Matyjaszewski, K.; Gaynor, S. G. *Macromolecules* **1997**, *30*, 7042.
(18) Mori, H.; Seng, D. C.; Lechner, H.; Zhang, M.; Müller, A. H. E. *Macromolecules* **2002**, *35*, 9270.
(19) Hawker, C. J.; Fréchet, J. M. J.; Grubbs, R. B.; Dao, J. *J. Am. Chem. Soc.* **1995**, *117*, 10763.
(20) Sunder, A.; Hanselmann, R.; Frey, H.; Mülhaupt, R. *Macromolecules* **1999**, *32*, 4240.
(21) Baskaran, D. *Macromol. Chem. Phys.* **2001**, *202*, 1569.
(22) Simon, P. F. W.; Radke, W.; Müller, A. H. E. *Makromol. Chem., Rapid Commun.* **1997**, *18*, 865.
(23) Sakamoto, K.; Aimiya, T.; Kira, M. *Chem. Lett.* **1997**, 1245.
(24) Webster, O. W.; Hertler, W. R.; Sogah, D. Y.; Farnham, W. B.; RajanBabu, T. V. *J. Am. Chem. Soc.* **1983**, *105*, 5706.
(25) Hertler, W. R.; Sogah, D. Y.; Webster, O. W.; Trost, B. M. *Macromolecules* **1984**, *17*, 1415.
(26) Dušek, K.; Šomvársky, J.; Smrcková, M.; Simonsick, W. J.; Wilczeck, L. *Polym. Bull. (Berlin)* **1999**, *42*, 489.
(27) Burgath, A.; Sunder, A.; Frey, H. *Macromol. Chem. Phys.* **2000**, *201*, 782.
(28) Galina, H.; Lechowicz, J. B.; Kaczmarski, K. *Macromol. Theory Simul.* **2001**, *10*, 174.
(29) Hölter, D.; Frey, H. *Acta Polym.* **1997**, *48*, 298.
(30) Radke, W.; Litvinenko, G. I.; Müller, A. H. E. *Macromolecules* **1998**, *31*, 239.
(31) Bharathi, P.; Moore, J. S. *Macromolecules* **2000**, *33*, 3212.
(32) Yan, D.; Müller, A. H. E.; Matyjaszewski, K. *Macromolecules* **1997**, *30*, 7024.
(33) Dicker, I. B.; Cohen, G. M.; Farnham, W. B.; Hertler, W. R.; Laganis, E. D.; Sogah, D. Y. *Macromolecules* **1990**, *23*, 4034.
(34) Middleton, W. J. *Org. Synth.* **1985**, *64*, 221.
(35) Jenkins, A. D.; Tsartolia, E.; Walton, D. R. M.; Horska-Jenkins, J.; Kratochvil, P.; Stejskaj, J. *Makromol. Chem.* **1990**, *191*, 2511.
(36) Lochmann, L.; Rodová, M.; Petránek, J.; Lím, D. *J. Polym. Sci., Polym. Chem. Ed.* **1974**, *12*, 2295.
(37) Lochmann, L.; Trekoval, J. *Makromol. Chem.* **1982**, *183*, 1361.
(38) Adler, H. J.; Lochmann, L.; Pokorny, S.; Berger, W.; Trekoval, J. *Makromol. Chem.* **1982**, *183*, 2901.
(39) Doskocilová, D.; Schneider, B.; Stoker, J.; Sevcik, S.; Prádny, M.; Lochmann, L. *Makromol. Chem* **1985**, *186*, 1905.
(40) Benoît, H.; Grubisic, Z.; Rempp, P.; Decker, D.; Zilliox, J. G. *J. Chem. Phys.* **1966**, *63*, 1507.
(41) Wintermantel, M.; Schmidt, M.; Becker, A.; Dorn, R.; Kühn, A.; Lösch, R. *Nachr. Chem. Technol. Lab.* **1992**, *40*, 331.
(42) Sanayei, R. A.; Suddaby, K. G.; Rudin, A. *Makromol. Chem.* **1993**, *194*, 1953.
(43) Litvinenko, G. I.; Simon, P. F. W.; Müller, A. H. E. *Macromolecules* **1999**, *32*, 2410.
(44) Müller, A. H. E. *Makromol. Chem., Macromol. Symp.* **1990**, *32*, 87.
(45) Brittain, W. J.; Dicker, I. B. *Macromolecules* **1989**, *22*, 1054.
(46) Yan, D.; Zhou, Z. *Macromolecules* **1999**, *32*, 819.
(47) Hölter, D.; Burgath, A.; Frey, H. *Acta Polym.* **1997**, *48*, 30.
(48) Müller, A. H. E.; Zhuang, R.; Yan, D. Y.; Litvinenko, G. *Macromolecules* **1995**, *28*, 4326.
(49) Stickler, M. Dissertation, Universität Mainz, 1977.

MA0358834